Cent. Eur. J. Phys. • 11(4) • 2013 • 431-439
DOI: 10.2478/s11534-013-0173-9

VERSITA

Central European Journal of **Physics**

Manipulation of atom-to-molecule conversion in a magnetic lattice

Research Article

Ning-Ju Hui[1], Li-Hua Lu[1]*, Li-Bin Fu[2], You-Quan Li[1]

1 *Department of Physics, Zhejiang University, Hangzhou 310027, China*

2 *Institute of Applied Physics and Computational Mathematics, Beijing 100088, China*

Received 12 October 2012; accepted 09 January 2013

Abstract: Atom-to-molecule conversion by the technique of optical Feshbach resonance in a magnetic lattice is studied in the mean-field approximation. For the case of a shallow lattice, we give the dependence of the atom-to-molecule conversion efficiency on tunnelling strength and atomic interaction by taking a double-well as an example. We find that one can obtain a high atom-to-molecule conversion by tuning the tunnelling and interaction strengths of the system. For the case of a deep lattice, we show that the existence of the lattice can improve the atom-to-molecule conversion for certain initial states.

PACS (2008): 03.75.Kk, 03.75.Lm, 03.75.Mn

Keywords: atom-to-molecule conversion • mean-field approximation • Feshbach resonance • magnetic lattice

1. Introduction

Since Bose-Einstein condensations (BECs) in dilute atomic gases were realized in 1995, the study of cold atoms has become a remarkable research area which has been extended from atomic to molecular systems in recent years. Molecular BECs are versatile not only for cold atomic physics but also for other research areas [1–3], because they include more degrees of freedom than atomic systems. To realize molecular BECs, one usually converts ultracold atoms into molecules through resonant photoassociation (optical Feshbach resonance) or magnetoassociation (magnetic Feshbach resonance) [4–11] rather than cool molecules directly. Additionally, besides the technique of Feshbach resonance, the stimulated Raman adiabatic passage technique was also used in the conversion of a Bose-Fermi mixture into molecules [12, 13]. In the above works, the atom-to-molecule conversion systems were all confined in a single well. Note that in recent experiments [14–17], satom-to-molecule conversion systems confined in an optical lattice have also been studied, where the atom-to-molecule conversion efficiency and the lifetime of molecules can be improved due to the suppression of inelastic collisions. Similar to optical lattices, magnetic lattices can also be expected to improve atom-to-molecule conversion since ultracold atoms were successfully transferred experimentally to a magnetic lattice potential in 2008 [18]. Compared with optical lattices,

*E-mail: lhlu@zju.edu.cn (Corresponding author)

magnetic lattices have several distinct advantages such as high stability with low technical noise and low heating rates, large and controllable barrier heights and others. It is thus meaningful to study the property of atom-to-molecule conversion in a magnetic lattice.

In this paper, we consider an atom-to-molecule conversion system in a magnetic lattice. In the mean field approximation, we study the influence of the magnetic lattice on the atom-to-molecule conversion efficiency and show how to improve the atom-to-molecule conversion. The rest of this paper is organized as follows. In Sect. 2, we present the model and the dynamical equations. In Sect. 3, we consider the case of a shallow lattice, *i.e.*, the atoms can tunnel between the nearest neighbouring sites. Taking a double-well as an example, we study the time evolution of molecular density and the effect of parameters of the system on the atom-to-molecule conversion. We also confirm our numerical results with the help of fixed points and energy contours of the system. In Sect. 4, we consider a deep lattice, *i.e.*, the atoms can not tunnel between the lattice sites. We show that the existence of the lattice can improve the atom-to-molecule conversion for certain initial states. In the last section, we give a brief summary and discussion.

2. Model and general formulation

We consider atom-to-molecule conversion via optical Feshbach resonance in a magnetic lattice, where the atoms are subject to the lattice but the molecules are not. The Hamiltonian describing such a system can be written as

$$\begin{aligned}\hat{H}_l = &-J\sum_{\langle i,j\rangle}(\hat{a}_i^\dagger\hat{a}_j+\hat{a}_j^\dagger\hat{a}_i)+\frac{\widetilde{U}_a}{2}\sum_i\hat{n}_{ai}(\hat{n}_{ai}-1)\\&+\frac{\widetilde{U}_b}{2}\hat{n}_b(\hat{n}_b-1)+\frac{\tilde{g}}{2}\sum_i(\hat{b}^\dagger\hat{a}_i\hat{a}_i\\&+\hat{b}\hat{a}_i^\dagger\hat{a}_i^\dagger)+\delta\hat{b}^\dagger\hat{b},\end{aligned}\tag{1}$$

where the operator $\hat{a}_{i(j)}^\dagger$ and $\hat{a}_{i(j)}$ creates and annihilates a bosonic atom in the $i(j)$th site separately and $\langle i,j\rangle$ denotes the two nearest neighbouring lattice sites, while $\hat{b}^\dagger$ and $\hat{b}$ creates and annihilates a bosonic molecule. They obey the commutation relation $[\hat{a}_i,\hat{a}_j^\dagger]=\delta_{ij}$ and $[\hat{b},\hat{b}^\dagger]=1$. Here the parameter J denotes the tunneling strength of atoms between the nearest neighbouring sites, which can be tuned by changing the distance between the neighbouring lattice sites or the height of the potential barrier separating the neighbouring lattice sites. $\widetilde{U}_a$ and $\widetilde{U}_b$ are the interaction strengths between the atoms and molecules, respectively. As we know, $\widetilde{U}_a=4\pi\hbar^2a_s/m$, where a_s is the s-wave scattering length and m is the atomic mass. The scattering length can be tuned by the optical Feshbach resonance technique. δ is the energy detuning between the atomic and molecular states, and $\tilde{g}$ refers to the coupling strength between atoms and molecules. The molecules in spin singlet state ($S=0$) are not subject to the magnetic lattice, so there is no subscript for b in the Hamiltonian (1).

In order to study the property of atom-to-molecule conversion, we need the dynamical equations of the system. The classical field description is an excellent approximation if the quantum fluctuation is small. As we know, the magnitude of quantum fluctuation around the condensate state scales down as $1/\sqrt{N}$ in zero temperature with N the particle number. There are usually 10^4-10^7 particles in dilute BEC experiments, so we adopt the mean-field description [19, 20]. In the mean field approximation, by replacing operators with their expectation values, *i.e.*, $\hat{a}_{i(j)}\to\langle\hat{a}_{i(j)}\rangle=\tilde{a}_{i(j)}$ and $\hat{b}\to\langle\hat{b}\rangle=\tilde{b}$, one can easily give the dynamical equations for $\tilde{a}_{i(j)}$ and $\tilde{b}$ with the help of Heisenberg equations of motion for $\hat{a}_{i(j)}$ and $\hat{b}$. These equations obey the conservation law $\sum_i\hat{a}_i^\dagger\hat{a}_i+2\hat{b}^\dagger\hat{b}=N$. To simplify the calculation, one usually assumes $a_{i(j)}=\tilde{a}_{i(j)}/\sqrt{N}$ and $b=\tilde{b}/\sqrt{N}$ with $\sum_i|a_i|^2+2|b|^2=1$. Then the dynamical equations for $a_{i(j)}$ and b can be rewritten as,

$$\begin{aligned}i\dot{a}_i &= -J(a_{i+1}+a_{i-1})+U_a|a_i|^2a_i+gba_i^*,\\ i\dot{b} &= U_b|b|^2b+\delta b+\frac{g}{2}\sum_i a_i^2,\end{aligned}\tag{2}$$

where $U_a=\widetilde{U}_aN$, $U_b=\widetilde{U}_bN$, $g=\tilde{g}\sqrt{N}$ and natural units have been used. Note that the interaction strength between molecules is much smaller than that between atoms in most experiments, so we ignore the interaction between molecules in the following calculation, *i.e.*, $U_b=0$. Meanwhile, the energy detuning is chosen as $\delta=0$. We study the atom-to-molecule conversion efficiency, which is defined as twice the density of the largest molecules $(2|b|^2_{max})$ in the time evolution, for the cases of a shallow lattice and deep lattice in the following two sections.

3. Shallow lattice

In this section, we consider that the atoms tunnel between the nearest neighbouring sites, *i.e.*, $J\neq0$. Although we can give the dynamical properties of the system for different lattice size L by solving (2) numerically, here we mainly take double-well as a typical example. For the

case of double-well, Eqs. (2) is simplified to,

$$\begin{aligned} i\dot{a}_1 &= -Ja_2 + U_a|a_1|^2 a_1 + gba_1^*, \\ i\dot{a}_2 &= -Ja_1 + U_a|a_2|^2 a_2 + gba_2^*, \\ i\dot{b} &= g(a_1^2 + a_2^2)/2, \end{aligned} \tag{3}$$

where $\delta = 0$ and $U_b = 0$ have been taken. Tunnelling strength J, atomic interaction strength U_a and the atom-molecule coupling strength g have the same dimensions. We choose g as unity and then all quantities are renormalized to be dimensionless.

3.1. Evolution and conversion efficiency

Now we are in a position to study the atom-to-molecule conversion of BECs in double wells with the help of (3). Here we consider the symmetrical initial state $a_{1,2} = \sqrt{1/2}$ and $b = 0$. We plot the time dependence of molecular density for different parameter values in Fig. 1 (a), (b) and the period of Rabi oscillation [21] versus U_a in Fig. 1 (c), (d). Fig. 1 (a) shows that all atoms can be converted into molecules and the system will always stay in the pure molecular state, *i.e.*, the oscillation period for this condition is infinite which corresponds to the peak in Fig. 1 (c). Whereas, from Fig. 1 (b), not all of atoms can be converted into molecules for some parameter values and the system is found to oscillate periodically. The oscillation period for this condition is finite, corresponding with the peak in Fig. 1 (d). The above results enlighten us in terms of choosing the appropriate parameter values for high atom-to-molecule conversion efficiency. So it is necessary to find a suitable relationship between thetunnelling strength J and atomic interaction strength U_a.

We plot the dependence of atom-to-molecule conversion efficiency on the atomic interaction strength in Fig. 2 (a) and (b), and on the tunnelling strength in Fig. 2 (c) and (d). Fig. 2 (a) and (b) show that for $J \neq 0$, the increase of interaction strength can improve the atom-to-molecule conversion when U_a is smaller than the critical value U_{ac}, while it suppresses the atom-to-molecule conversion when $U_a > U_{ac}$, which is different from the case of $J = 0$ plotted in Fig. 5 (b). Additionally, for a given value of J, when $U_a = U_{ac}$, one can get the highest atom-to-molecule conversion efficiency which is dependent on the value of J. Comparing Fig. 1 (c) and (d) with Fig. 2 (a) and (b), we find that both the periods of Rabi oscillation versus U_a and the dependence of the maximum atom-to-molecule conversion efficiency on U_a exhibit a similar behaviour and they have the same parameters of the peaks, *e.g.*, $J = 0.5g$, $U_a = 2g$ for Fig. 1 (c) and Fig. 2 (a) and $J = g$, $U_a = 3.853g$ for Fig. 1 (d) and Fig. 2 (b). When $J = 0.5g$ and $U_a = 2g$, all of the atoms can be converted into molecules and stay in the pure molecular final state with infinite period. While only some of the atoms can be converted into molecules and the period is finite with parameter values $J = g$ and $U_a = 3.853g$. Fig. 2 (c) and (d) tell us that for the case of $U_a \neq 0$, the dependence of atom-to-molecule conversion efficiency on the tunnelling strength does not change monotonically; rather, there is a critical value J_c where the atom-to-molecule conversion efficiency is the highest.

In order to further describe the overall dependence of atom-to-molecule conversion on the strengths of tunnelling and interaction of the system, we plot the projection of the atom-to-molecule conversion efficiency in the J-U_a plane in Fig. 3 (a). The purple filled point $(\mathcal{J}_c, \mathcal{U}_{ac}) = (g/\sqrt{2}, 2\sqrt{2}g)$ in Fig. 3 (a) is an important critical point called a "general critical point". When $J < \mathcal{J}_c$, all of the atoms can be converted into molecules if the parameter values are selected according to the red solid line, *i.e.*, $U_a = 4J$. On the other hand, for the case of $J > \mathcal{J}_c$, although not all of the atoms can be converted into molecules no matter what parameter values are taken, one can also get higher atom-to-molecule conversion by taking the parameter values on the red dotted line which deviates from the line $U_a = 4J$ (*i.e.*, the black dashed line). Fig. 3 shows that both the atomic interaction and tunnelling strength can affect the atom-to-molecule conversion efficiency and one can get high conversion by tuning the parameters of the systems properly. In order to convert all atoms into molecules, one should choose the parameter values on the red solid line, *i.e.*, $U_a = 4J$ and $J < \mathcal{J}_c$.

Additionally, we extend our study to the triple-well case and give the projection of the atom-to-molecule conversion efficiency in the J-U_a plane in Fig. 3 (b). There is also a general critical point $(\mathcal{J}_c, \mathcal{U}_{ac}) = (g\sqrt{2}/4, 3\sqrt{2}g)$ and the relation of the red solid line is $U_a = 12J$ as $J < \mathcal{J}_c$. The analysis of the dependence of atom-to-molecule conversion efficiency on U_a, J and the oscillated period is similar to the double-well case.

3.2. Fixed points and energy analysis

In order to understand the dependence of conversion efficiency on the parameters J and U_a, we study the properties of the fixed points. By expressing $a_i = \sqrt{\rho_{ai}}e^{\theta_{ai}}$ and $b = \sqrt{\rho_b}e^{\theta_b}$, we can write Eq. (3) as

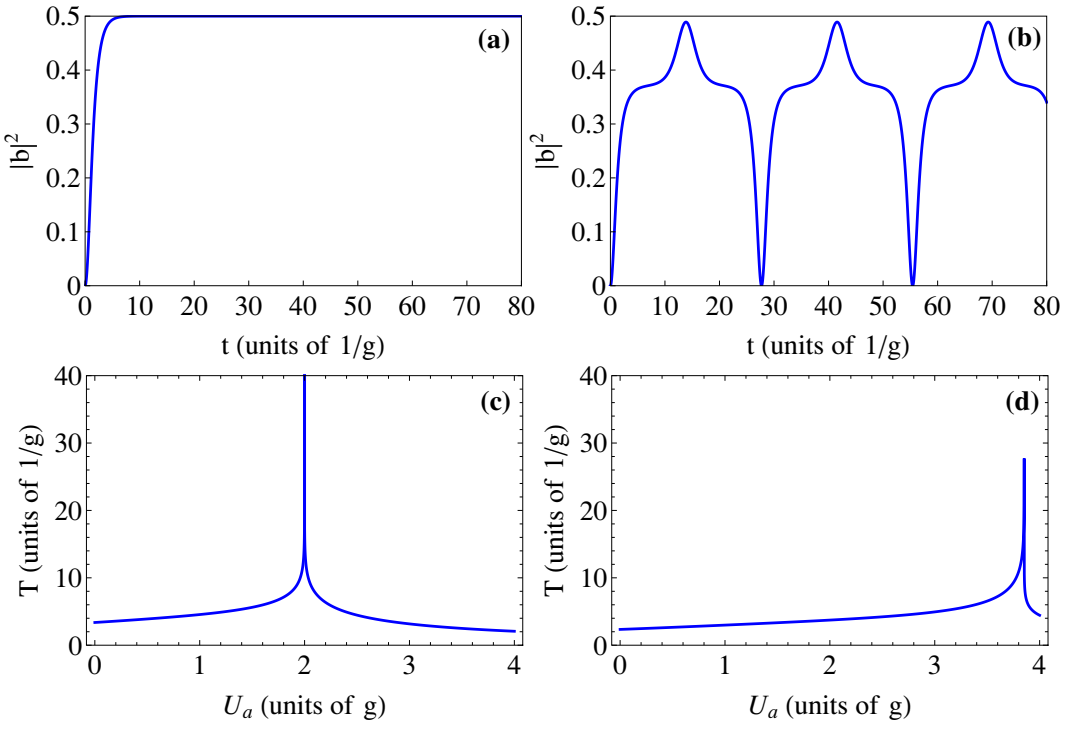

Figure 1. (Colour online) Time dependence of the molecular density with symmetrical initial conditions in (a) and (b). The parameter values are $J = 0.5g$ and $U_a = 2g$ (a), $J = g$, $U_a = 3.853g$ (b). Period of Rabi oscillation T versus U_a in (c) and (d). The parameter values are $J = 0.5g$ (c) and $J = g$ (d).

$$
\begin{aligned}
\dot{z} &= -2J\sqrt{(1-2\rho_b)^2 - z^2}\sin(2\phi_a) - g\sqrt{\rho_b}\Big[(1-2\rho_b+z)\sin(\phi-2\phi_a) - (1-2\rho_b-z)\sin(\phi+2\phi_a)\Big],\\
\dot{\phi}_a &= \frac{Jz}{\sqrt{(1-2\rho_b)^2 - z^2}}\cos(2\phi_a) + \frac{g}{2}\sqrt{\rho_b}\Big[\cos(\phi-2\phi_a) - \cos(\phi+2\phi_a)\Big] + \frac{U_a}{2}z,\\
\dot{\rho}_b &= \frac{g}{2}\sqrt{\rho_b}\Big[(1-2\rho_b+z)\sin(\phi-2\phi_a) + (1-2\rho_b-z)\sin(\phi+2\phi_a)\Big],\\
\dot{\phi} &= \frac{2J(1-2\rho_b)}{\sqrt{(1-2\rho_b)^2 - z^2}}\cos(2\phi_a) - g\sqrt{\rho_b}\Big[\cos(\phi-2\phi_a) + \cos(\phi+2\phi_a)\Big] - U_a(1-2\rho_b)\\
&\quad + \frac{g}{4\sqrt{\rho_b}}\Big[(1-2\rho_b+z)\cos(\phi-2\phi_a) + (1-2\rho_b-z)\cos(\phi+2\phi_a)\Big],
\end{aligned}
\tag{4}
$$

where the constant $N = \rho_{a1} + \rho_{a2} + 2\rho_b$ has been used and $z = \rho_{a1} - \rho_{a2}$, $\phi_a = (\theta_{a2} - \theta_{a1})/2$, $\phi = \theta_{a1} + \theta_{a2} - \theta_b$. z and ϕ_a, ρ_b and ϕ are mutually canonical conjugations, respectively. They satisfy the Hamiltonian canonical equation, *i.e.*, $\dot{z} = -\partial H_{cl}/\partial\phi_a$, $\dot{\phi}_a = \partial H_{cl}/\partial z$, $\dot{\rho}_b = -\partial H_{cl}/\partial\phi$ and $\dot{\phi} = \partial H_{cl}/\partial\rho_b$. The corresponding classical Hamiltonian of the system is given by

$$
\begin{aligned}
H_{cl} &= -J\sqrt{(1-2\rho_b)^2 - z^2}\cos(2\phi_a) + \frac{U_a}{4}\Big[(1-2\rho_b)^2 + z^2\Big]\\
&\quad + \frac{g}{2}\sqrt{\rho_b}\Big[(1-2\rho_b+z)\cos(\phi-2\phi_a) + (1-2\rho_b-z)\cos(\phi+2\phi_a)\Big].
\end{aligned}
$$

We should note that the time evolution of the system can be determined by the classical Hamiltonian due to the energy conservation law. According to Ref. [19], the dy-

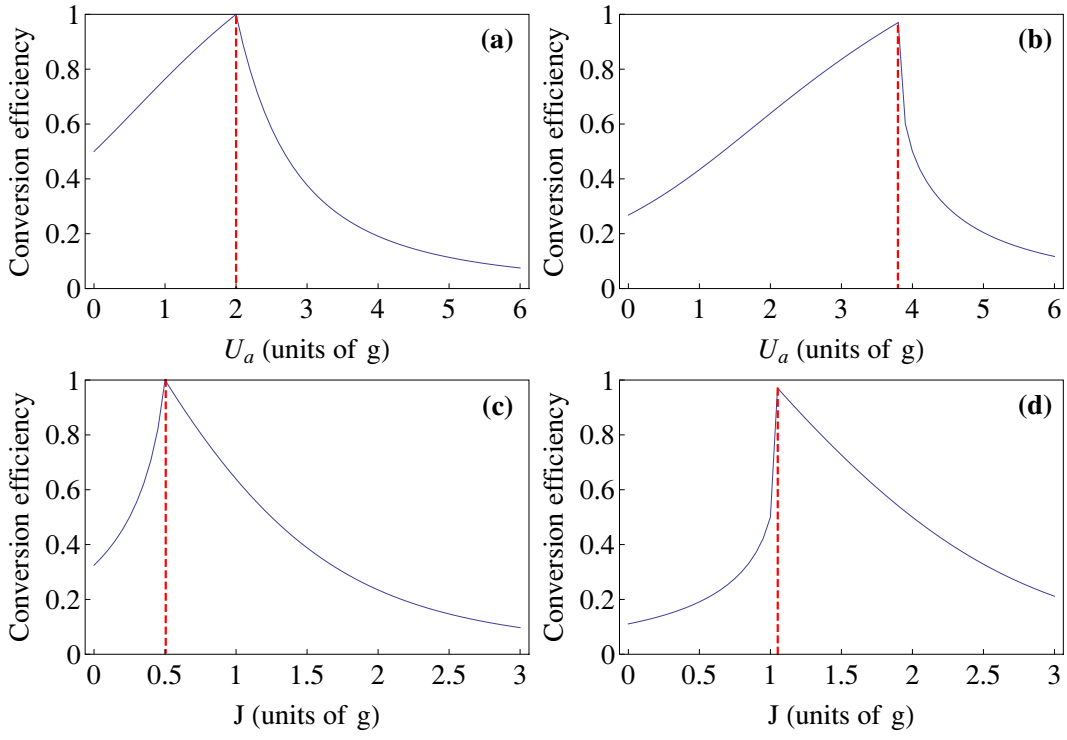

Figure 2. (Colour online) Dependence of atom-to-molecule conversion efficiency on the atomic interaction strength (a) , (b) and tunnelling strength (c), (d) for a double-well. The parameter values are $J = 0.5g$ (a), $J = g$ (b), $U_a = 2g(c)$, and $U_a = 4g(d)$. The vertical pink dashed lines are guides to the eye.

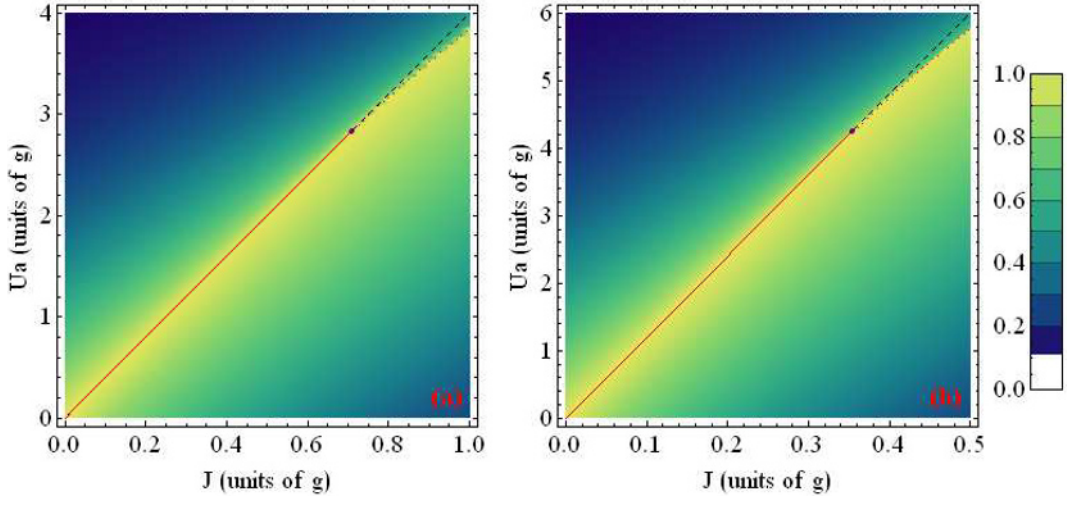

Figure 3. (Colour online) Projection of the atom-to-molecule conversion efficiency in the J-U_a plane for the cases of a double-well (a) and triple-well (b). The red solid line and red dotted line distinguish the complete and incomplete conversions respectively. The purple filled points are the general critical point. The black dashed lines are $U_a = 4J$ (a) and $U_a = 12J$ (b) which are guides to the eye.

namical system in double wells described by Eq. (3) is non-integrable due to the existence of atom-to-molecule conversion. So it can be used to study some fascinating phenomena such as instability and chaos which have been studied in the triple-well system without atom-to-molecule conversion [22, 23]. Additionally, the complex dynamical behaviors, both stable and unstable, of lattice bosonic models have been investigated [24–26]. Note that

we consider the integrable regime with conditions $z = 0$ and $\phi_a = 0$ and describe the regular motions with symmetrical initial conditions in this paper. In order to get the fixed point solutions, we set $\dot{z} = 0$, $\dot{\phi}_a = 0$, $\dot{\rho}_b = 0$ and $\dot{\phi} = 0$ in Eq. (4). For the initial states $z = 0$, $\phi_a = 0$, the atomic distribution and phase in the double wells are the same at any time, *i.e.*, $z(t) = 0$ and $\phi_a(t) = 0$. Since these conditions are selected, the Eq. 4 become dynamical equations for a pair of mutually canonical conjugations. Then the fixed points are determined by the following equations:

$$\begin{aligned} g\sqrt{\rho_b}(1-2\rho_b)\sin\phi &= 0, \\ 2J - U_a(1-2\rho_b) + \frac{g(1-6\rho_b)}{2\sqrt{\rho_b}}\cos\phi &= 0. \end{aligned} \tag{5}$$

The conditions for the fixed points are written as $\dot{\rho}_b = \dot{\phi} = 0$. Here we do not write the fixed point solutions in order to save space, although we can get such solutions through solving Eq. (5). Note that when $0 \leq J \leq g/\sqrt{2}$, there is a fixed point $\rho_b = 1/2$ with ϕ being not well defined. Since the fixed point $\rho_b = 1/2$ exists for the case of $0 \leq J \leq g/\sqrt{2}$, it is possible for the system to reach it, *i.e.*, all of the atoms can be converted into molecules by tuning the parameters of the system properly. According to Eq. (5), we know that the energy of the system is $-J+U_a/4$ for the initial state we considered, and zero for the fixed point $\rho_b = 1/2$. So if the system can reach the fixed point $\rho_b = 1/2$, the parameters must satisfy $-J + U_a/4 = 0$ due to the existence of the energy conservation law. This explains why the conversion efficiency corresponding to the parameter values taken on the red line in Fig. 3 is 1. Whereas, for the case of $J > g/\sqrt{2}$, the fixed point $\rho_b = 1/2$ disappears, and then not all of the atoms can be converted into molecules, no matter what atomic interaction strength is taken, which is confirmed by Fig. 2 (b).

In Fig. 4, we plot the energy contours in the phase space of ρ_b and ϕ for the two cases of $J < g/\sqrt{2}$ and $J > g/\sqrt{2}$, respectively. From Fig. 1 (a) and (b), we can see that, for a fixed value of J, one can get the highest atom-to-molecule conversion efficiency when $U_a = U_{ac}$. So in Fig. 4, we take the atomic interaction strength as U_{ac} which is determined by J. Note that we can obtain $U_{ac} = 4J$ analytically for $J < g/\sqrt{2}$, while the value of U_{ac} needs to be determined by numerical methods for $J > g/\sqrt{2}$. For the initial states we considered, the system evolves along the pink dashed curve. Fig. 4 (a1) and (b1) further confirm that the system can reach the state $\rho_b = 1/2$ for $J < g/\sqrt{2}$, but clearly cannot for $J > g/\sqrt{2}$.

We also study the properties of the fixed points to confirm the dependence of the conversion efficiency on the parameters J and U_a for the triple-well from Fig. 3 (b) and they are in good agreement. The fixed point $\rho_b = 1/2$ exists for the case of $0 \leq J \leq g\sqrt{2}/4$ when the atoms can be converted into molecules completely with corresponding critical interaction strength, while the fixed point $\rho_b = 1/2$ disappears for the case of $J > g\sqrt{2}/4$ when only part of the atoms can be combined to molecules.

4. Deep lattice

In this section, we consider the case of a deep lattice, where the height of the potential barrier separating the neighbouring sites is so high that we can ignore the tunnelling of atoms between neighbouring sites, *i.e.*, $J = 0$. For a deep lattice without atom-to-molecule conversion, the ground state has a fixed number of particles per lattice site, and the relative phase between lattice sites is smeared out. However, the existence of atom-to-molecule conversion, where the molecules are not subject to the lattice, makes the phases between lattice sites related and well defined. In order to study the atom-to-molecule conversion efficiency, we assume there is no molecule in the system at the initial time and the atoms are equally populated in the lattice, *i.e.*, the initial state is $b = 0$ and $a_i = \sqrt{N/L}$ with L is the number of lattice sites. Once the initial state is fixed, we can get the time evolution of the system by solving Eq. (2) numerically and the dependence of the atom-to-molecule conversion efficiency on the atomic interaction strength U_a if the value of L is not very large. We summarize our results in Fig. 5 (a) and (b) for the cases of $L = 1, 2, 3, 4$.

In Fig. 5 (a), we plot the time dependence of molecular density for different L with certain atomic interaction strength ($U_a = 2g$), and plot the corresponding dependence of the atom-to-molecule conversion efficiency on the atomic interaction strength U_a in Fig. 5 (b). The molecular density oscillating periodically with time for any value of L is displayed in Fig. 5 (a). The larger the number of lattice sites, the longer the oscillation period. From Fig. 5 (b), we find that the atom-to-molecule conversion efficiency becomes smaller when the atomic interaction strength increases. For the same atomic interaction strength, the atom-to-molecule conversion efficiency becomes higher with the increase of the number of lattice sites, which shows that one can improve atom-to-molecule conversion by a magnetic lattice even if the atomic interaction strength is fixed.

In order to confirm the above numerical results, we study the system with analytical methods. For the symmetrical initial state $a_i = 1/\sqrt{L}$ and $b = 0$, the lattice sites are equivalent, *i.e.*, the values of a_i at any time do not change with different i. Then we can introduce $A = a_i\sqrt{L}$.

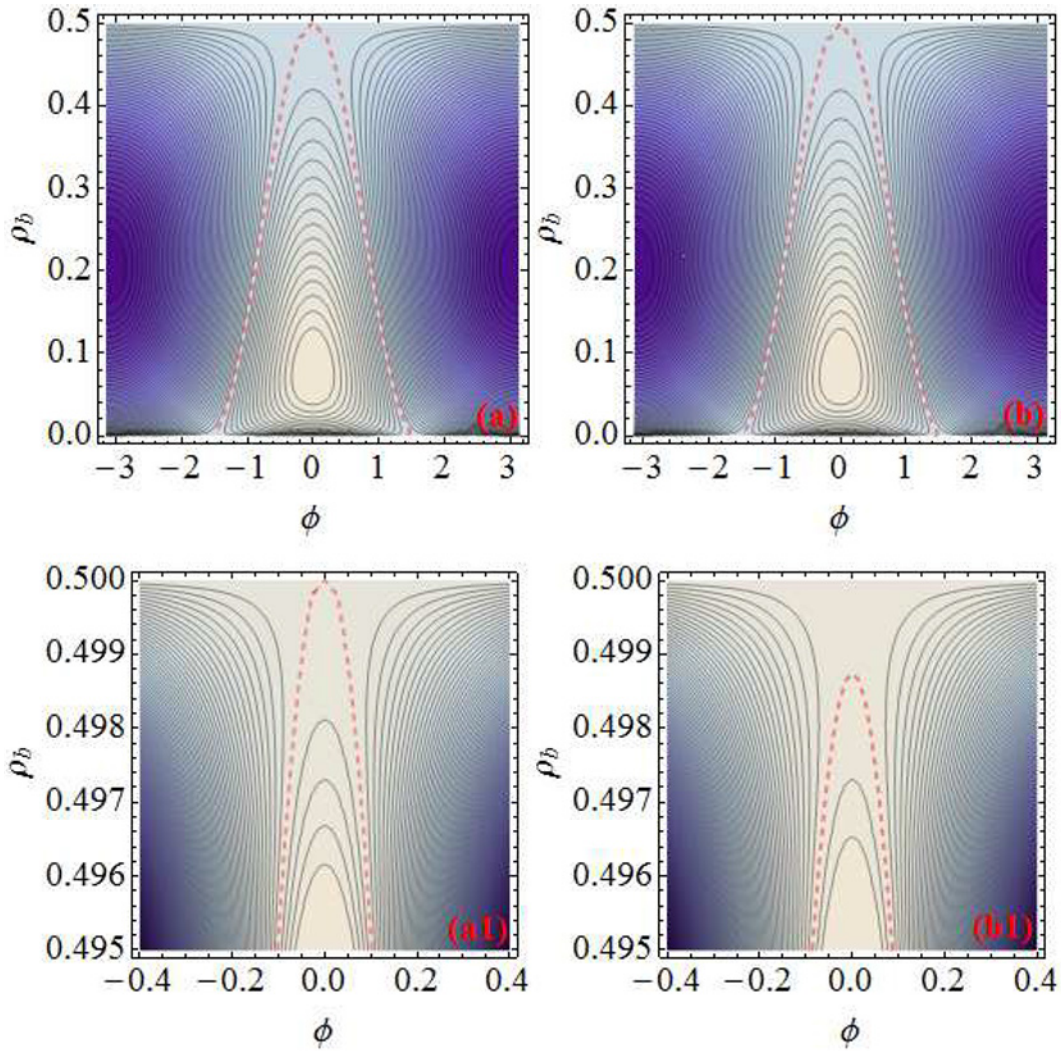

Figure 4. (Colour online) Energy contour in the phase space of ϕ and ρ_b. The parameters are $J = 0.707$ and $U_a = 2.828$ (a), $J = 0.708$ and $U_a = 2.832$ (b). The enlargements of the small blue boxes in (a) and (b) are (a1) and (b1), respectively. The pink dashed curves correspond to the energy with the initial states $a_1 = a_2 = 1/\sqrt{2}$ and $b = 0$.

Substituting this definition into Eq. (2), we can give the dynamical equation for A and b:

$$\begin{aligned} i\dot{A} &= \frac{U_a}{L}|A|^2A + gbA^*, \\ i\dot{b} &= \frac{g}{2}A^2, \end{aligned} \tag{6}$$

with the particle conservation law $|A|^2+2|b|^2 = 1$. Eq. (6) is similar to the dynamical equation for atom-to-molecule conversion system in a single well except for the rescale of the atomic interaction strength. From Eq. (6), we can see that equally distributing the same atomic BEC into a magnetic lattice can reduce the effective interaction strength between atoms for the case of $J = 0$ by comparing with the case of a single well. Additionally, we know that the existence of atomic interaction can suppress atom-to-molecule conversion, which can be confirmed by Fig. 5 (b). So for the same atomic interaction strength, the existence of a deep magnetic lattice can improve atom-to-molecule conversion. Because the effective atomic interaction strength is U_a/L, the larger the number of lattice sites is, the higher the atom-to-molecule conversion efficiency will be. We only consider the symmetrical initial state above. For the asymmetrical initial state, *i.e.*, the initial atomic distributions $|a_i(0)|^2$ are not the same, the existence of a deep magnetic lattice can also improve the atom-to-molecule conversion if the initial phases of a_i are the same. Time dependence of molecule density for different values of L and dependence of the atom-

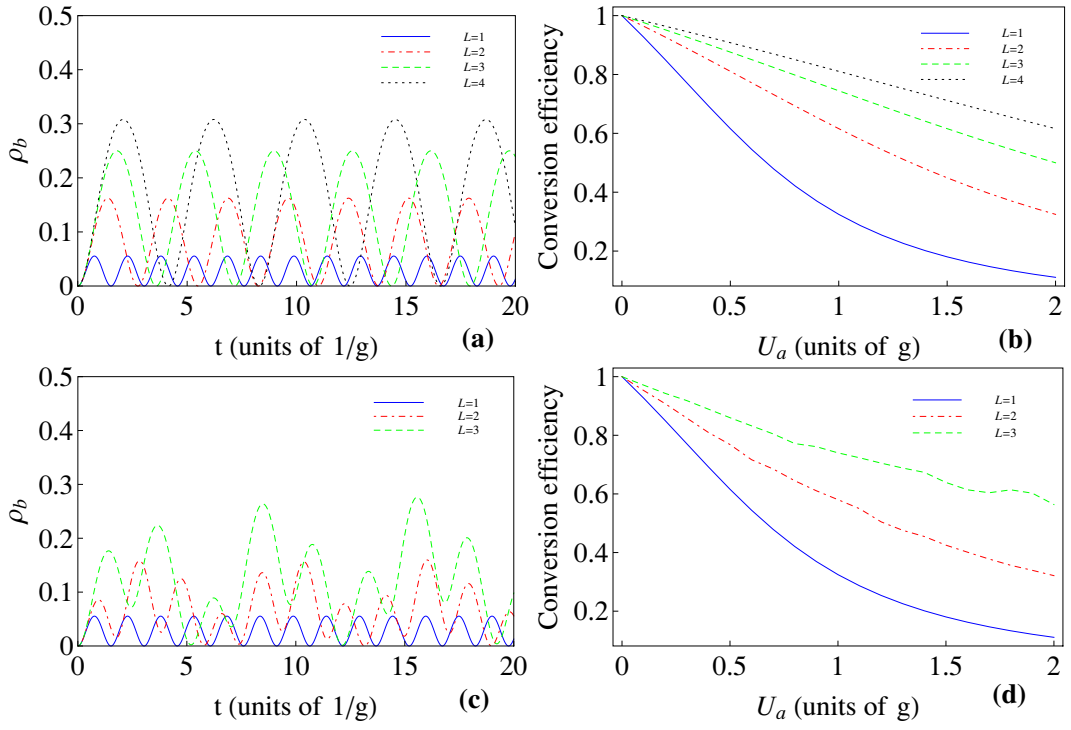

Figure 5. (Colour online) Time dependence of molecular density for different values of L with symmetrical initial state (a) and asymmetrical initial state (c), dependence of the atom-to-molecule conversion efficiency on the atomic interaction strength U_a for different L with symmetrical initial state (b) and asymmetrical initial state (d). The parameter values are $U_a = 2g$ and $J = 0$ (a) and (c), $J = 0$ (b) and (d). The asymmetrical initial conditions considered are $|a_1(0)|^2 = 1/4$, $|a_2(0)|^2 = 3/4$, $|b(0)|^2 = 0$ for $L = 2$ and $|a_1(0)|^2 = 1/4$, $|a_2(0)|^2 = 1/4$, $|a_3(0)|^2 = 1/2$, $|b(0)|^2 = 0$ for $L = 3$.

to-molecule conversion efficiency on the atomic interaction strength with asymmetrical initial state are shown with Fig. 5 (c) and (d). The asymmetrical initial states $|a_1(0)|^2 = 1/4$, $|a_2(0)|^2 = 3/4$, $|b(0)|^2 = 0$ for adouble-well and $|a_1(0)|^2 = 1/4$, $|a_2(0)|^2 = 1/4$, $|a_3(0)|^2 = 1/2$, $|b(0)|^2 = 0$ for a triple-well are considered. However, for the case of initial a_i with different phases, the lattice cannot always improve the atom-to-molecule conversion. We should note that the phases of the condensates between lattice sites are well defined in the Mott insulator state for the existence of atom-to-molecule conversion. The phases of the condensates between lattice sites remain unchanged if they are the same initially. However, the phases of the atomic condensates between lattice sites will evolve over time if they are different initially.

5. Summary and discussion

In this paper, we have studied atom-to-molecule conversion in a magnetic lattice. For a shallow lattice, where the atomic tunnelling strength J is unneglected, we studied the effect of tunnelling and interaction strengths of the system on atom-to-molecule conversion by taking the double-well case as an example. We gave the dependence of the atom-to-molecule conversion efficiency on the tunnelling strength of atoms and the atomic interaction for the double-well and triple-well cases. The general critical points for both cases were found. We also showed that atoms could be converted into molecules completely if one chose appropriate parameter values, *i.e.*, the parameters on the red solid lines in Fig. 3 (a) and (b) while not completely with other parameter values. Analysis of fixed points and the energy contours confirmed the results. The integrable regime with $z = \phi_a = 0$, which corresponds to regular motion has been discussed. As to the other regime, where unstable dynamical behavior may occur, we refer to Ref. [24–26], in which stable and unstable dynamical behaviors in the 3-mode bosonic models in an optical lattice without atom-to-molecule conversion have been studied extensively. For a deep lattice, where the atomic tunnelling strength J is neglected, we showed that if the initial phases of BECs in different lattice sites were equal, the existence of lattice sites improved atom-to-molecule conversion. Considering a symmetrical initial state, we showed that the larger the number of lattice sites

is, the higher the atom-to-molecule conversion efficiency that can be reached. We also confirmed our results by an analytical method with the help of the redefinition of a_i. In summary, we gave some suggestions on how to obtain higher conversion efficiency with suitable relationship between tunnelling and interaction strengths.

Acknowledgment

This work is supported by NSFC Grant No. 10674117, No. 11074216, No. 11104244, Zhejiang NSFC Grant No.Y4110063, and partially by PCSIRT Grant No. IRT0754.

References

[1] C. A. Regal, M. Greiner, D. S. Jin, Phys. Rev. Lett. 92, 040403 (2004)
[2] R. V. Krems, Int. Rev. Phys. Chem. 24, 99 (2005)
[3] V. V. Flambaum, M. G. Kozlov, Phys. Rev. Lett. 99, 150801 (2007)
[4] C. A. Regal, C. Ticknor, J. L. Bohn, D. S. Jin, Nature 424, 47 (2003)
[5] K. E. Strecker, G. B. Partridge, R. G. Hulet, Phys. Rev. Lett. 91, 080406 (2003)
[6] J. Herbig et al., Science 301, 1510 (2003)
[7] K. Xu, T. Mukaiyama, J. R. Abo-Shaeer, J. K. Chin, D. E. Miller, W. Ketterle, Phys. Rev. Lett. 91, 210402 (2003)
[8] S. Dürr, T. Volz, A. Marte, G. Rempe, Phys. Rev. Lett. 92, 020406 (2004)
[9] K. M. Jones, E. Tiesinga, P. D. Lett, P. S. Julienne, Rev. Mod. Phys. 78, 483 (2006)
[10] T. Köhler, K. Góral, P. S. Julienne, Rev. Mod. Phys. 78, 1311 (2006)
[11] C. Chin, R. Grimm, P. Julienne, E. Tiesinga, Rev. Mod. Phys. 82, 1225 (2010)
[12] K.-K. Ni et al., Science 322, 231 (2008)
[13] L. H. Lu, Y. Q. Li, Phys. Rev. A 76, 053608 (2007)
[14] G. Thalhammer et al., Phys. Rev. Lett. 96, 050402 (2006)
[15] T. Volz et al., Nature Phys. 2, 692 (2006)
[16] T. Stöferle, H. Moritz, K. Günter, M. Köhl, T. Esslinger, Phys. Rev. Lett. 96, 030401 (2006)
[17] J. G. Danzl et al., Nature Phys. 6, 265 (2010)
[18] M. Singh et al., J. Phys. B: At. Mol. Opt. Phys. 41, 065301 (2008)
[19] R. Franzosi, V. Penna, Phys. Rev. A 65, 013601 (2001)
[20] Y. Khodorkovsky, G. Kurizki, A. Vardi, Phys. Rev. A 80, 023609 (2009)
[21] X. Q. Xu, L. H. Lu, Y. Q. Li, Phys. Rev. A 80, 033621 (2009)
[22] M. Johansson, J. Phys. A: Math. Gen. 37, 2201 (2004)
[23] P. Jason, M. Johansson, K. Kirr, Phys. Rev. E 86, 016214 (2012)
[24] R. Franzosi, V. Penna, Phys. Rev. E 67, 046227 (2003)
[25] B. Liu, L. B. Fu, S. P. Yang, J. Liu, Phys. Rev. A 75, 033601 (2007)
[26] T. F. Viscondi, K. Furuya, J. Phys. A: Math. Theor. 44, 175301 (2011)